Nonlinear Control of a Fully-Fed Variable Speed Pumped Storage Plant

Janailson Lima, Gilney Damm, Abdelkrim Benchaib, Emilia Nobile, Alexander Schwery

Nonlinear Control of a Fully-Fed Variable Speed Pumped Storage Plant

Janailson R. Lima * **Gilney Damm** ** **Abdelkrim Benchaib** *
Emilia Nobile *** **Alexander Schwery** ***

* *SuperGrid Institute, Villeurbanne, 69611 France (e-mail: janailson.rodrigues, abdelkrim.benchaib@ supergrid-institute.com).*
** *Université d'Evry Val d'Essonne, (e-mail: gilney.damm@l2s.centralesupelec.fr).*
*** *GE Renewable Energy, (e-mail: emilia.nobile, alexander.schwery@GE.com).*

Abstract: This paper presents the nonlinear control of a Fully-Fed Synchronous Machine based Variable Speed Pumped Storage Plant (FFSM PSP). First, a model is developed and the control objective is established followed by the control design. The control algorithm is designed using Feedback Linearization robustified by a Second Order Sliding Mode Control (SOSMC). Using both techniques allows a fast response of the system while relaxing the conditions on the Sliding Mode Control and avoiding the known chattering problem. The control is compared with the industrial standard PI controller from the dynamic response point of view and also during short-circuits.

Keywords: Application of power electronics, Control system design, Control of renewable energy sources, Power systems stability, Modeling and simulation of power systems.

1. INTRODUCTION

Pumped storage plants (PSP) are one of the most reliable and well-known large storage solutions in the power grid (Ibrahim et al. (2008)). Pumping water to the upper reservoir during low consumption periods and producing energy during peaks of consumption for hundreds of years (see Fig. 1). They are, however, reaching the limit of the exploitable sites (Deane et al. (2010)) while at the same time new challenges in the power system require more flexibility than the past decades. Nowadays, with the insertion of intermittent renewable energies, the response of a PSP needs to be faster than before (Ngoc et al. (2009)). Another challenge for the PSP is to increase their penetration knowing that the best economic exploitable sites are already taken (Deane et al. (2010)).

The Variable Speed PSP is seen today as the answer for both problems: it can increase PSP insertion. The speed variation allows a bigger operation range, increasing the number of technically feasible and economically attractive sites (Belhadji et al. (2013)). From the dynamic point of view, using the power electronics to control the power output of the turbine allows the PSP to react rapidly to any perturbation in the network (Pannatier (2010)).

Concerning the control of a Variable Speed PSP, few works have addressed this problem. In Hodder (2004), a controller for the whole chain of a PSP was designed for a Doubly-Fed Induction Machine based Variable Speed PSP (DFIM PSP). The author used two cascaded control loops: an inner control loop that controls either the current of the machine or the current in the transformer, and an outer control loop. The outer control loop controls an internal DC link while the inner controls: the reactive power and either the active power or the turbine's speed. The control design performed by Hodder (2004) is based on the transfer function approach using Méplat and Symmetric optimum criteria. Pannatier (2010) used the controllers developed in Hodder (2004) to assess the different strategies and its impacts on the operation of the DFIM PSP and their capability to provide services to the power grid.

DFIM PSP uses a wounded rotor induction machine with an Alternate Current (AC) excitation system. When using this technology, part of the power proportional to the speed variation goes through the excitation. The speed variation of this solutions is then limited by the rated power of the excitation system. Compared to the DFIM PSP, the Fully-Fed Synchronous Machine based Variable Speed PSP (FFSM PSP) is more flexible and robust. Synchronous Machine are the most used machines for power generation and is, thus a mastered technology. Additionally, for the FFSM PSP, the maximum speed variation is determined by the mechanical limits of the pump-turbine. However, due to higher prices and size of the converters, FFSM PSP is mostly used in low power applications. Nevertheless, due to tighter requirements from power system operators, the use of FFSM PSP is increasing since the machine is decoupled from the power system (Steimer et al. (2014)).

The present work focuses on the nonlinear control of the converters in a FFSM PSP. The chosen control approach is a cascaded one. Hence, the objective here is not to change the control methodology developed by Hodder (2004) and Pannatier (2010), but give a different way to design the controllers. Also, the cascaded control allows the use of

different time scales in the systems as well as the plug and play characteristic (see Chen (2015)). Controllers were implemented in SIMSEN and simulated using turbine data from software library. SIMSEN is a software developed by the Ecole Polytechnique Federale de Laussanne (EPFL) which simulates hydraulic and electromagnetic phenomena.

From the control point of view, the FFSM PSP is controlled by the voltages in its two converters. One of them is connected to the power grid through a transformer (Grid Side Converter - GSC) and the other to the machine (Machine Side Converter - MSC). The converters are connected through a DC capacitance in what is called back-to-back connection to each other. Since the voltage output of the converters depends on the DC Voltage of the capacitor (which is also a state), the relation between control input and state is not linear. Simulation results in accordance to theory show that the nonlinear approach is more suitable for the FFSM PSP.

2. FFSM PSP MODEL AND CONTROL PROBLEM

The original complete model of the system is obtained from the different subsystems present in the FFSM PSP (see Fig. 1). A change of variables can be applied (as shown in the following) to the original model in order to ease the control design and highlight interesting properties from the control point of view. The subsystems to be taken into account when modeling the FFSM PSP are:

- The grid side converter (GSC) also called front end converter
- The machine side converter (MSC) also called the back end converter
- The DC link voltage dynamics
- The Machine rotational speed
- The Hydraulic circuit

The model shown here will concern the electric part of the system, i.e., both converters and the DC link between them, as well as the speed of the machine (see Fig. 1). Since no control is developed for the turbine, the hydraulic part is not modeled nor discussed in this paper. Nevertheless it is considered, for control purpose, that there is a control input in the turbine represented by the water gate opening. For more details on the hydraulic part, consult Pannatier (2010) or Nicolet (2007).

2.1 Grid Side Converter (GSC) Model

This model can also be found in Hodder (2004) and is based on the XR model of the transformer connected to the GSC (see Fig. 1) in pu:

$$\frac{di_t}{dt} = \omega_b \left(V_{tr} - \frac{R_{SC}}{X_{SC}} i_t + j\omega_j i_t - \frac{1}{X_{SC}} M_t \cdot V_{DC} \right) \quad (1)$$

Where i_t is the complex current through the transformer ($i_t = i_{td} + j i_{tq}$). The nominal frequency of the network in rad/s is represented by ω_b. R_{SC} and X_{SC} are respectively the short-circuit resistance and reactance of the transformer. ω_j and V_2 are the frequency and the voltage of the transformer at the converter side. M_t is the duty cycle of the PWM, i.e., the control variable at the converter. V_{DC} is the DC voltage in the capacitance.

2.2 Machine Side Converter (MSC) Model

The model of the MSC is given by the equations of the machine and is represented in Fig. 1. In Damm (2001) a complete model of the synchronous machine is developed with different number of states for different purposes. For the control design it was chosen the third order model taking into account direct and quadrature axis flux as well as the excitation. However, for simulation, it was considered a fifth order model with damper windings in quadrature and direct axis. From the stability point of view, this simplification is not a concern since the damper winding improve the stability of the synchronous machine (see Damm (2001)).

$$\begin{aligned} v_d &= r_s i_d + \frac{1}{\omega_N}\frac{d\Phi_d}{dt} - \omega\Phi_q \\ v_f &= r_f i_f + \frac{1}{\omega_N}\frac{d\Phi_f}{dt} \\ v_q &= r_s i_q + \frac{1}{\omega_N}\frac{d\Phi_q}{dt} + \omega\Phi_d \end{aligned} \quad (2)$$

$$\begin{aligned} \Phi_d &= x_d i_d + x_{df} i_f \\ \Phi_f &= x_{df} i_d + x_f i_f \\ \Phi_q &= x_q i_q \end{aligned} \quad (3)$$

Where the indexes s, d, q, N and f are referred, respectively, to the stator, the d and q axis, the nominal value and field circuit. The variables v, r, i, ω and Φ are, respectively, the voltages, electric circuit's resistance, current, speed and electromagnetic fluxes.

Since current is a measurable variable and it will be used for the first control loop it was explicitly put as a state. A change of variables is made using equations 3. Additionally, the index m is added to the machine side current in order to differentiate it from the current in the transformer (i_t).

$$\begin{aligned} \frac{di_{md}}{dt} &= \frac{\omega_N}{x_f\left(x_d x_f - x_{df}^2\right)}\left(\left(r_f x_{df}^2 + r_s x_f^2\right)\cdot i_{md}\right. \\ &\quad + x_{df} x_f \cdot V_{exc} - r_f x_f \cdot \Phi_{exc} - x_q x_f^2 \cdot \omega \cdot i_{mq} \\ &\quad \left. - x_f^2 \cdot M_d \cdot V_{DC}\right) \\ \frac{di_{mq}}{dt} &= \omega_N \left(\left(-\frac{x_d}{x_q} + \frac{x_{df}^2}{x_q x_f} \right) \cdot \omega \cdot i_{md} - \frac{r_s}{x_q} i_{mq} \right. \\ &\quad \left. + \frac{1}{x_q} M_q V_{DC} - \frac{x_{df}}{x_q x_f} \cdot \omega \Phi_{exc} \right) \\ \frac{d\Phi_{exc}}{dt} &= \omega_N \left(\frac{r_f x_{df}}{x_f} i_{md} - \frac{r_f}{x_f} \Phi_{exc} + V_{exc} \right) \end{aligned} \quad (4)$$

It can be seen that the field current is not used as state variable. This because it is considered that the excitation of the machine is regulated by a classical excitation controller (not developed in this paper).

2.3 DC Link Model

The DC link is represented by the capacitance and its dynamics (see Fig. 1) in pu:

$$\begin{aligned} \frac{dV_{DC}}{dt} &= \frac{1}{2H_c}\left(-i_{td}\cdot M_{td} - i_{tq}\cdot M_{tq}\right. \\ &\quad \left. + i_{md}\cdot M_{md} + i_{mq}\cdot M_{mq}\right) \end{aligned} \quad (5)$$

Where H_c is the electrostatic inertia of the DC link in seconds given by $H_c = C_{tot} V_0^2 / 2 S_N$. M_{td}, M_{tq}, M_{md} and

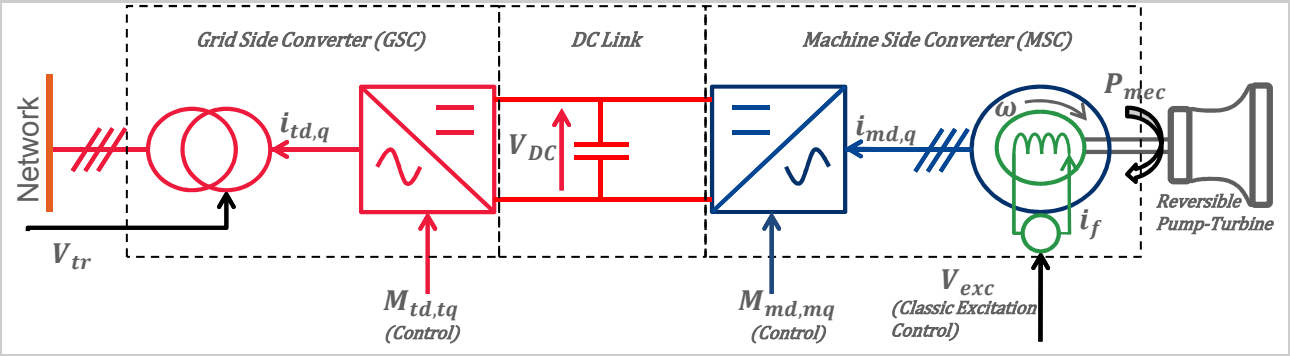

Fig. 1. Scheme of the electric part of a Fully-Fed Synchronous Machine based Variable Speed PSP with its state variables and inputs.

M_{mq} are the duty cycles of the two converters. The indexes t and m stand for transformer and machine's circuits, respectively. d and q are the perpendicular axis obtained from the park transform.

One can also obtain the following electrostatic energy expression after some mathematical manipulation:

$$\frac{dW_{DC}}{dt} = \frac{1}{H_c}\left(P_{IN} - P_{OUT}\right) = \frac{1}{H_c}\left(-P_t + P_{mac}\right) \quad (6)$$

Where, $V_{DC}^2 = W_{DC}$ (pu), and since V_{DC} is only considered as positive ($V_{DC} \in \mathbb{R}_+$), the change of coordinates is invertible. The power of the transformer is given by $P_t = V_{trd}i_{td} + V_{trq}i_{tq}$ as presented previously. The power of the machine can be calculated using $P_{mac} = \omega \cdot \Phi_{exc} \cdot i_{mq}$. This last model is more suitable for nonlinear control design than the first one.

2.4 Angular Speed Model

The rotating speed model is based on the sum of positive and negative torque that will accelerate or decelerate the machine rotating speed in pu. Thus, neglecting the local friction and considering the sign convention adopted by SIMSEN:

$$\frac{d\omega}{dt} = \frac{1}{2H_j}\left(-T_{elec} + T_{mec}\right) \quad (7)$$

Where ω is the rotating speed of the group rotor plus pump/turbine. H_J is the inertia constant of the group in seconds given by $H_J = J_{tot}\omega_0^2/2S_N$. T_{elec} and T_{mec} are the electrical and mechanical torque produced by the machine and the turbine respectively and defined below. For control design, it is considered that the mechanical torque can be controlled by the hydraulic side.

Similar to the capacitance and electrostatic energy model, one can develop an equivalent model between angular speed and kinetic energy:

$$\frac{dW_K}{dt} = \frac{1}{H_J}\left(P_{IN} - P_{LOAD}\right) = \frac{1}{H_J}\left(-P_{mac} + P_{Mec}\right) \quad (8)$$

Where P_{mac} is the as defined in the previous section and P_{Mec} is the mechanical power input of the turbine (prime mover). In the following both controllers will be developed: kinetic energy controller and speed controller.

2.5 Complete Model and Control Problem

The complete model can then be stated as:

$$\begin{aligned}
\frac{di_{td}}{dt} &= \omega_b\left(V_{trd} - \frac{R_{SC}}{X_{SC}}\cdot i_{td} + \omega_j i_{tq} - \frac{1}{X_{SC}}M_{td}\sqrt{W_{dc}}\right)\\
\frac{di_{tq}}{dt} &= \omega_b\left(V_{trq} - \frac{R_{SC}}{X_{SC}}i_{tq} - \omega_j i_{td} - \frac{1}{X_{SC}}M_{tq}\sqrt{W_{dc}}\right)\\
\frac{dW_{dc}}{dt} &= \frac{1}{H_c}\left(-V_{trd}i_{td} - V_{trq}i_{tq} + \sqrt{W_K}\cdot\Phi_{exc}\cdot i_{md}\right)\\
\frac{di_{md}}{dt} &= \frac{\omega_N}{x_f\left(x_d x_f - x_{df}^2\right)}\left(\left(r_f x_{df}^2 + r_s x_f^2\right)\cdot i_{md} + x_{df}x_f\cdot V_{exc} - r_f x_f\cdot\Phi_{exc} - x_q x_f^2\cdot\sqrt{W_K}\cdot i_{mq} - x_f^2\cdot M_{md}\cdot\sqrt{W_{DC}}\right)\\
\frac{di_{mq}}{dt} &= \omega_N\left(\left(-\frac{x_d}{x_q} + \frac{x_{df}^2}{x_q x_f}\right)\cdot\sqrt{W_K}\cdot i_{md} - \frac{r_s}{x_q}i_{mq} + \frac{1}{x_q}M_{mq}\sqrt{W_{dc}} - \frac{x_{df}}{x_q x_f}\sqrt{W_K}\cdot\Phi_{exc}\right)\\
\frac{d\Phi_{exc}}{dt} &= \omega_N\left(\frac{r_f x_{df}}{x_f}i_{md} - \frac{r_f}{x_f}\Phi_{exc} + V_{exc}\right)\\
\frac{dW_K}{dt} &= \frac{1}{H_J}\left(-\sqrt{W_K}\cdot\Phi_{exc}\cdot i_{mq} + P_{Mec}\right)
\end{aligned} \quad (9)$$

The main objective of the FFSM PSP control is to regulate the following Outputs:

1. Rotational Speed
2. Machine's Reactive Power Output
3. DC Link Voltage
4. GSC Reactive Power Output
5. FFSM PSP Active Power Output to the Network

Using the following Control Inputs:

1. Water Gate Opening
2. Machine's Excitation Voltage
3. MSC's direct axis voltage

4. MSC's quadrature axis voltage
5. GSC's direct axis voltage
6. GSC's quadrature axis voltage

In this model, voltages generated by the converters are represented as a multiplication of DC voltage times a duty cycle. Also, it is considered that all the states are measurable as well as the outputs.

Regarding the water gate opening and the excitation of the machine, neither of their control design is discussed in this paper. For simulation, a standard excitation controller from SIMSEN was used in the machine. For the turbine governor a PID controller was used (see Kundur et al. (1994) for more on hydro turbine's control).

Concerning active power, there are three different control modes named after the variable controlled by the MSC: Active Power Control Mode, DC Voltage Control Mode and Angular Speed Control Mode. Once the control objective of the MSC is defined, the control objectives of the GSC and the turbine are fixed.

3. FFSM PSP NONLINEAR CONTROL DESIGN

In this section, the design of the controllers for the converters is performed. The MSC and GSC are separated by the DC Link, hence it is possible to design the controllers independently. Moreover, since the control loops are cascaded, it is possible to design the inner current control loop and then integrate it to the design of the outer control loop.

Control Algorithm: The controller is designed following a Feedback Linearization (FL) technique. FL technique erases all nonlinearities of the model, but is not very robust to parametric and model errors. The controller is then robustified by a Sliding Mode Control (SMC). SMC is a technique robust to model and parametric errors, and guarantees finite time convergence to the designed surface. On the other hand, it is known that discontinuities in SMC may cause chattering problems. Chattering is a high frequency phenomenon mainly caused by delays in SMC applications (see Khalil and Grizzle (1996) and Isidori (2013) for further details in FL and SMC).

To avoid chattering, different types of SMC were proposed (see e.g. Sira-Ramirez (1993)). In the present work, a Second-Order Sliding Mode Control (SOSMC) was used. Using this technique, the control input is no longer discontinuous while maintaining the desired robustness to parametric and model errors. Furthermore, to avoid the calculation of higher order derivatives of the surface and still guarantee finite time convergence, the Super-Twisting Algorithm (STA) was used (Fridman and Levant (2002), Pisano (2000)). The following paragraphs detail the control design with further development on the FL-STA SOSMC algorithm used.

Current Control Loop Design: The FL-SOSMC design was applied for all control modes of the FFSM PSP. Except the Active and Reactive Power controllers which include an integrator to avoid static error. For the sake of conciseness, the control design of the current control loop of the GSC in Active Power Mode is used as example. The other control designs are omitted but were designed using the same methodology.

With the current model presented in (9), it is possible to design a feedback model of the control for the current control loop of the GSC. Here, for example, we take the d axis current controller, but similar methodology can be applied to other controllers.

From Eq. 9:

$$x = [i_{td} \quad i_{tq} \quad i_{md} \quad i_{mq}]^T$$

$$f(x) = \begin{bmatrix} \omega_b \left(V_{trd} - \frac{R_{SC}}{X_{SC}} i_{td} + \omega_j i_{tq} \right), \\ \omega_b \left(V_{trq} - \frac{R_{SC}}{X_{SC}} i_{tq} - \omega_j i_{td} \right), \\ \frac{\omega_N}{x_f \left(x_d x_f - x_{df}^2 \right)} \left(\left(r_f x_{df}^2 + r_s x_f^2 \right) \cdot i_{md} \right. \\ + x_{df} x_f \cdot V_{exc} - r_f x_f \cdot \Phi_{exc} \\ \left. - x_q x_f^2 \cdot \sqrt{W_K} \cdot i_{mq} \right), \\ \omega_N \left(\left(-\frac{x_d}{x_q} + \frac{x_{df}^2}{x_q x_f} \right) \cdot \sqrt{W_K} \cdot i_{md} \right. \\ \left. - \frac{r_s}{x_q} i_{mq} - \frac{x_{df}}{x_q x_f} \sqrt{W_K} \cdot \Phi_{exc} \right) \end{bmatrix} \quad (10)$$

$$g(x) = diag \left(-\frac{\omega_b}{X_{SC}} \sqrt{W_{dc}}, \quad -\frac{\omega_b}{X_{SC}} \sqrt{W_{dc}}, \right. \\ \left. \frac{\omega_N x_f}{\left(x_d x_f - x_{df}^2 \right)} \sqrt{W_{dc}}, \quad \frac{\omega_N}{x_q} \sqrt{W_{dc}} \right)$$

$$u = [M_{td} \quad M_{tq} \quad M_{md} \quad M_{mq}]^T$$

The current model can be represented by the form $\dot{x} = f(x) + g(x)u$, allowing the following Feed Back Linearization:

$$u = g^{-1} \cdot (-f(x) + v_k), \quad k = td, tq, md, mq \quad (11)$$

A sufficient condition is the existence of $g^{-1}(x)$ which is always true since $W_{DC} > 0$. Considering that $f(x)$ and $g(x)$ are not exactly known due to neglected dynamics (e.g. damper windings, PWM dynamics) or parametric errors. The real values of those functions will not be correctly calculated by the controller. The real feedback is then designed using functions $\hat{f}(x)$ and $\hat{g}(x)$ which may, or not, be equal to the real functions. Thus, the new closed loop model with FL control is given by:

$$\dot{i} = f(x) - \hat{f}(x) \cdot g(x) \cdot \hat{g}^{-1}(x) + g(x) \cdot \hat{g}^{-1}(x) \cdot v \quad (12)$$

With the auxiliary control input $v = [v_{td} \quad v_{tq} \quad v_{md} \quad v_{mq}]^T$ where one can apply the super-twisting algorithm for SOSMC according to Pisano (2000).

$$\begin{aligned} v_k &= -\lambda_k \cdot |e_k|^{1/2} sgn(e_k) + v_{1k} \\ \dot{v}_{1k} &= -\alpha_{1k} sgn(e_k) \end{aligned} \quad (13)$$

$e = [e_k]$, $k = td, tq, md, mq$, is the sliding vector to be defined. In the present work, the individual sliding surfaces are defined as the error between the state and its reference value $e_k = i_k - i_{k,ref}$. The main advantage of using both, FL and SOSMC techniques is that the conditions for convergence of the super-twisting algorithm are now related to the values of:

$$\begin{aligned} a(x) &= f(x) - \hat{f}(x) \cdot g(x) \cdot \hat{g}^{-1}(x) \\ b(x) &= g(x) \cdot \hat{g}^{-1}(x) \end{aligned} \quad (14)$$

Where $a(x)$ and $b(x)$ are the model errors. Thus, for suitable positive constant U_{Mk}, C_k, K_{Mk} and K_{mk}, it is possible to show that:

$$|\dot{a}_k(x)| + |\dot{b}_k(x)|U_{Mk} < C_k, \quad 0 \leq K_{mk} \leq b(x) \leq K_{Mk} \quad (15)$$

The parameters for the SOSMC must satisfy the following conditions:

$$\begin{aligned} \alpha_k &> \frac{C_k}{K_{mk}} \\ \lambda_k &> \sqrt{\frac{2}{K_{mk}\alpha_k - C_k}} \frac{(K_{mk}\alpha_k + C_k)\, K_{Mk}}{K_{mk}^2} \end{aligned} \quad (16)$$

The main result of this paper can be summarized by the following Theorem:

Theorem 1. The Control Algorithm performed by 11 and 13 under conditions 15 and 16 drive the system to the sliding surface e in finite time.

The controllers were put together and simulated for validation of the control design.

4. SIMULATIONS AND RESULTS

To validate the proposed controllers and methodology, it was implemented and simulated on SIMSEN to compare the control performance with previous controllers. SIMSEN is a software developed by Ecole Polytechnique Federale de Laussane (EPFL). It can simulate transient phenomena in hydro and electrical systems and is considered as the industrial standard for detailed simulations of hydro plants. More information on SIMSEN can be found in Nicolet (2007).

From the dynamic point of view, it can be seen in Fig. 2 that the nonlinear controller has a behavior similar to a first order system while the linear controller has some overshoot. Hence the main advantages of the nonlinear controllers from the dynamic point of view are: faster response without overshoot and easier tuning of control parameters (see Section 3.0.2).

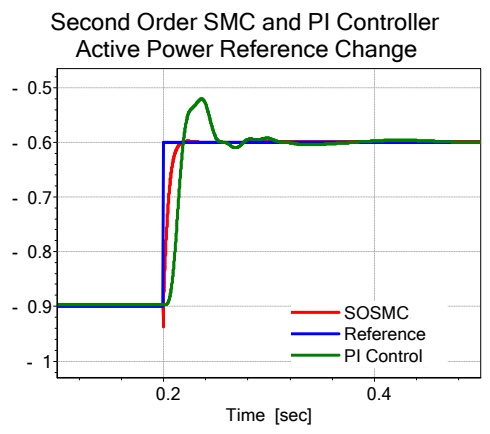

Fig. 2. Response for a step in Reference Active Power Output (blue): comparison between Nonlinear (red) and Linear (dark green) Controller

To validate the robustness of the proposed controller when compared to the linear one, their performances during a three phase short-circuit are compared. This simulation is done based on the Low Voltage Ride-Through (LVRT) requirement. The LVRT is a voltage vs time profile which defines the minimum required capability of a generator to withstand a voltage dip (ENTSO-E (2013)). It is perhaps the most difficult requirement imposed by the grid code, and was simulated by a three-phase short-circuit at the point of common coupling (PCC) of the FFSM PSP with the power network. For validation purpose, it is considered that the short-circuit is cleared in 150ms.

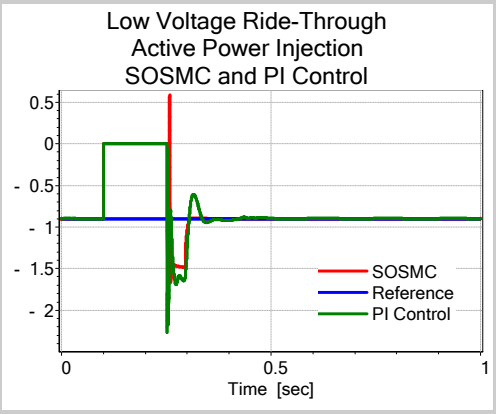

Fig. 3. Active Power Output after a short-circuit at the point of common coupling: comparison between Nonlinear (red) and Linear (dark green) Controller.

Fig. 3 shows the Active Power output of the GSC during the short-circuit. As it can be seen, during the short-circuit the power coming from the MSC cannot be transmitted to the power network. Once the voltage comes back, there is an overshoot on the nonlinear control, but the controller has a smoother recovery phase.

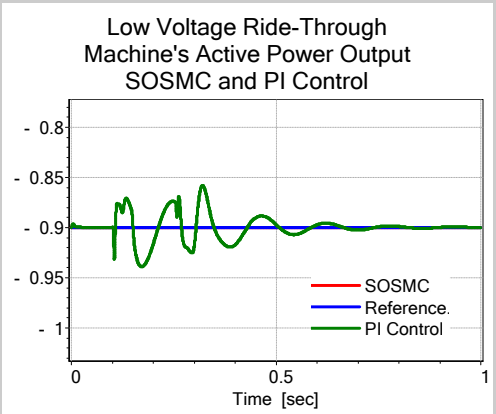

Fig. 4. Machine's Active Power Output after a short-circuit at the point of common coupling: comparison between Nonlinear (red) and Linear (dark green) Controller

The most important difference can be seen, however, in Fig. 4. When using the developed nonlinear controller, the short-circuit has zero impact in the machine. The same is not true for the linear control that shows oscillations in

power. Both controllers are still robust as expected from the FFSM architecture, but it is clear that the nonlinear controller is more robust to short-circuits than the linear one.

Additionally, the controllers were compared to their robustness for parametric error. Fig. 5 shows the same response as Fig. 2 now with 40% parametric error in the DC capacitance value. As one can see, the PI controller is unstable while the nonlinear one has the same performances. Moreover, it indicates that by using a nonlinear control, it is possible to achieve stability for lower values of the capacitance, reducing costs on the converter design.

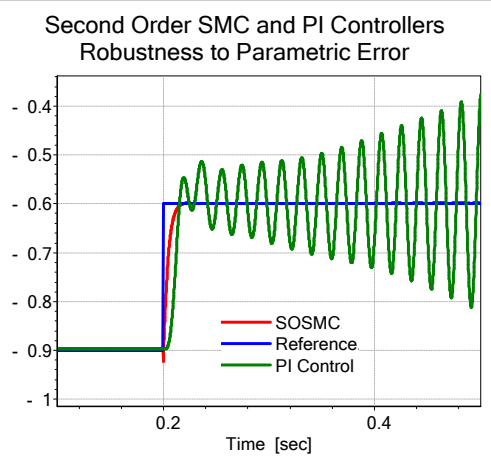

Fig. 5. Response for a step in Reference Active Power Output (blue): comparison between Nonlinear (red) and Linear (dark green) Controller for 40% error in one of the parameters.

Finally, with the nonlinear control design developed here, control tuning is simplified when compared to the PI controller. In practice, control parameters shown in (13) are lower bounded by (15) and (16) and upper bounded by control limits and chattering.

5. CONCLUSIONS

In the present paper, the nonlinear control of a Fully-Fed Synchronous Machine based Variable Speed Pumped Storage Plant (FFSM PSP) is designed. The control is designed using Feed-Back Linearization (FL) and Second Order Sliding Mode Control (SOSMC) for higher robustness and speed of the controller.

The proposed controller is compared with the industrial standard linear control designed using the symmetric and Méplat's optimum criteria. The proposed controller is more robust during short-circuits as it is validated through simulations.

With the proposed controller, it is possible to determine the limits of robustness for a set of parameters. Moreover, results have shown that when using the nonlinear controller, a short-circuit on the transformer/network side does not affect the machine.

The control is also more robust to parametric errors and allows a reduction on the size of the DC capacitance. Additionally, practical control tuning is simplified when using the limits given by the Super-Twisting Algorithm.

REFERENCES

Belhadji, L., Bacha, S., Munteanu, I., Rumeau, A., and Roye, D. (2013). Adaptive mppt applied to variable-speed microhydropower plant. *IEEE Transactions on Energy Conversion*, 28(1), 34–43.

Chen, Y. (2015). *Nonlinear Control and Stability Analysis of Multi-Terminal High Voltage Direct Current Networks*. Ph.D. thesis, Université Paris Sud-Paris XI.

Damm, G. (2001). *Contributions to the Stabilization of Power Generators*. Ph.D. thesis, Université Paris XI.

Deane, J.P., Gallachóir, B.Ó., and McKeogh, E. (2010). Techno-economic review of existing and new pumped hydro energy storage plant. *Renewable and Sustainable Energy Reviews*, 14(4), 1293–1302.

ENTSO-E (2013). Requirements for grid connection applicable to all generators. *European Network of Transmission System Operators for Electricity, ENTSO-E (2013 March)*.

Fridman, L. and Levant, A. (2002). Higher order sliding modes. *Sliding mode control in engineering*, 11, 53–102.

Hodder, A. (2004). *Double-Fed Asynchronous Moto-Generator Equipped with a 3-Level VSI Cascade*. Ph.D. thesis, Ecole Polytechnique Fdrale de Laussane.

Ibrahim, H., Ilinca, A., and Perron, J. (2008). Energy storage systemscharacteristics and comparisons. *Renewable and sustainable energy reviews*, 12(5), 1221–1250.

Isidori, A. (2013). *Nonlinear control systems*. Springer Science & Business Media.

Khalil, H.K. and Grizzle, J. (1996). *Nonlinear systems*, volume 3. Prentice hall New Jersey.

Kundur, P., Balu, N.J., and Lauby, M.G. (1994). *Power system stability and control*, volume 7. McGraw-hill New York.

Ngoc, P.D.N., Pham, T.T.H., Bacha, S., and Roye, D. (2009). Optimal operation for a wind-hydro power plant to participate to ancillary services. In *Industrial Technology, 2009. ICIT 2009. IEEE International Conference on*, 1–5. IEEE.

Nicolet, C. (2007). *Hydroacoustic Modelling and Numerical Simulation of Unsteady Operation of Hydroelectric Systems*. Ph.D. thesis, Ecole Polytechnique Fdrale de Laussane.

Pannatier, Y. (2010). *Optimisation des stratgies de Rglage d'une Installation de Pompage Turbinage Vitesse Variable*. Ph.D. thesis, Ecole Polytechnique Fdrale de Laussane.

Pisano, A. (2000). *Second Order Sliding Modes: Theory and Applications*. Ph.D. thesis, Universitá degli Studi de Cagliari.

Sira-Ramirez, H. (1993). On the dynamical sliding mode control of nonlinear systems. *International journal of control*, 57(5), 1039–1061.

Steimer, P.K., Senturk, O., Aubert, S., and Linder, S. (2014). Converter-fed synchronous machine for pumped hydro storage plants. In *Energy Conversion Congress and Exposition (ECCE), 2014 IEEE*, 4561–4567. IEEE.